6-1992

Groundwater Flow in a Compressible Unconfined Aquifer with Uniform Circular Recharge

Vitaly A. Zlotnik
University of Nebraska-Lincoln, vzlotnik1@unl.edu

Glenn Ledder
University of Nebraska-Lincoln, gledder1@unl.edu

WATER RESOURCES RESEARCH, VOL. 28, NO. 6, PAGES 1619–1630, JUNE 1992

Groundwater Flow in a Compressible Unconfined Aquifer With Uniform Circular Recharge

VITALY ZLOTNIK

Department of Geology, University of Nebraska, Lincoln

GLENN LEDDER

Department of Mathematics, University of Nebraska, Lincoln

The distributions of the hydraulic head and velocity components of the transient groundwater flow in an unconfined compressible aquifer of finite thickness under constant uniform circular recharge are obtained from the linearized mathematical model by the use of integral transforms. The result generalizes Dagan's (1967) solution which was derived by neglecting the compressibility. By treating the compressibility parameter as a small value, the formula for the hydraulic head is analyzed by asymptotic methods, resulting in approximations to the exact solutions for the head and velocities on small and large time scales. The hydraulic head and flow velocities can be accurately approximated by Dagan's formula for large times; for small times, neglecting the compressibility gives a large relative error but small absolute error.

1. INTRODUCTION

The interaction between groundwater flow systems, water supply wells, and natural or artificial groundwater recharge creates a complex velocity flow field in aquifers. This velocity field can be represented as a result of the interaction of vertical line sinks (wells) and horizontal areal sources (recharge). The flow is three dimensional rather than two dimensional and is transient rather than steady. Thus, to study contaminant transport below the water table, a three-dimensional unsteady model is necessary to delineate major contaminant pathways.

The role of groundwater flow modeling is to provide an estimate of the flow velocities. Head predictions are of little interest. Velocity estimates, however, are usually based on hydraulic head differences and therefore are much more sensitive to numerical modeling errors than are estimates of the hydraulic head alone. Satisfactory predictions of transport often require that the velocity field be calculated on a fine spatial grid. Therefore analytical solutions have some advantage over numerical procedures. Unfortunately, such solutions are not often available for cases of practical importance [*National Research Council*, 1990].

In this paper we consider the flow induced in an unconfined compressible aquifer of finite depth by an areal source (a source of finite horizontal extent), as illustrated in Figure 1. Such sources represent groundwater recharge for the problems of transport of agricultural fertilizers [*Dillon*, 1989], oil spills from underground storage tanks [*Levy et al.*, 1990], and leachates from landfills [*Ostendorf et al.*, 1989]. In the near field of the contamination source the velocity field is predominantly vertical, as contaminants are submerged into deeper layers of an unconfined aquifer; farther from the source, the velocity direction changes sharply from predominantly vertical to predominantly horizontal [*Hunt*, 1971].

Experimental results confirm the Dupuit assumption for the elevation of the groundwater mound under a source area [*Hantush*, 1967], provided the rise of the water table relative to the initial saturated thickness of the aquifer is as high as 50%. This assumption is frequently used in engineering practice when the shape and volumetric characteristics of the groundwater mound are of interest [*Morel-Seytoux et al.*, 1990]. However, this approach does not provide realistic estimates for groundwater flow velocities. As far as we know, the only analytical three-dimensional solution available is that obtained for an unconfined incompressible aquifer with areal circular recharge [*Dagan*, 1967]. That analysis does not present the velocity distribution. The solution was derived under the following assumptions: (1) that the ratio of recharge (I) to hydraulic conductivity (K_v) is a small parameter and (2) that the specific yield of the aquifer is not appreciably changed by the recharge. The problem was linearized using I/K_v as a small parameter. Green's functions were then used to obtain the solution for the hydraulic head.

To analyze the influence of the small parameter I/K_v and the applicability of the linearized solution for the full nonlinear problem, *Lennon et al.* [1979] applied the numerical boundary integral method. The numerical simulation showed that the linearized, incompressible, constant-specific-yield solution underpredicts the groundwater mound rise for large times in aquifers with thicknesses less than 2–10 times the recharge radius if the small parameter approaches the value 0.2. However, there was no analysis about the influence of compressibility of the unconfined aquifer or the influence of flow in the unsaturated zone on the development of water mounds.

The effect of compressibility for flow caused by a well (vertical line sink) has been shown to be significant for very early stages of pumping, causing delayed response of drawdown in an unconfined aquifer [*Neuman*, 1974, 1979]. "Dagan's method does not take into account the phenomenon of delayed gravity response, and therefore it is limited in its application to relatively large distances from the pumping well and to sufficiently large values of time, at which the

Paper number 92WR00462.
0043-1397/92/92WR-00462$05.00

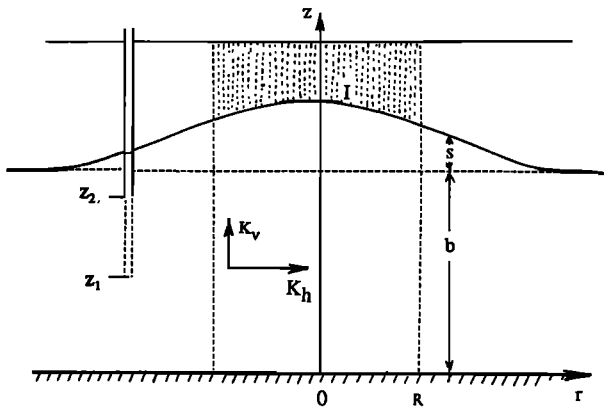

Fig. 1. Schematic diagram of groundwater recharge in an unconfined aquifer of finite thickness.

effect of elastic storage is very small" [*Neuman*, 1975, p. 329].

In this paper we consider the effect of compressibility on flow induced by areal recharge. We obtain the general solution for the compressible case and so determine the effect of compressibility by comparing the compressible solution to that obtained by Dagan. We are thus able to discuss the error made by using the incompressible solution to approximate the solution in the compressible case.

According to *Kroszinsky and Dagan* [1975] and *Brutsaert and El-Kadi* [1984], the unsaturated zone above the water table has little quantitative effect on drawdown in the case of an aquifer with coarse soil structure. We consider only the saturated zone in this work. A model which could address the influence of the unsaturated zone would be outside the scope of the linearized theory.

In the problem discussed in this paper there are two small parameters that must be considered. The ratio of specific recharge to conductivity will be taken to be small throughout the following analysis, so that the effect of the other parameter can be studied within the framework of the linearized theory. The ratio of storativity to specific yield (σ) will be used as a small parameter to obtain useful approximations.

Under the assumptions of the linearized theory we obtain an analytical three-dimensional solution for the hydraulic head and spatial flow velocity components in an unconfined, compressible, homogeneous, anisotropic aquifer under the influence of low-intensity groundwater recharge by a constant source uniformly distributed over a finite circular region. The results appear in the form of definite integrals, which we evaluate numerically. We also obtain an approximate solution for the compressible case by asymptotic expansion of the exact solution followed by asymptotic matching. The resulting approximation is virtually indistinguishable from the exact solution but has a simpler form and is therefore of great value in obtaining an analytic comparison of the incompressible and compressible solutions. Further analysis yields simple approximate quantitative statements of the long-term effect of compressibility on the hydraulic head and spatial flow velocity components for all near-field locations.

2. Problem Statement

We begin by writing down and solving the problem for the increase of hydraulic head over the initial level in an unconfined aquifer under a circular source of recharge. The velocity vector can then be obtained as the gradient of the hydraulic head. The model will be solved exactly, but the solution is somewhat complicated. We then derive approximate solutions on two different time scales from the exact solution and use the method of matched asymptotic expansions (see, for example, *Murdock* [1991]) to obtain an approximate solution valid for all time. This uniform approximation can be used in place of the exact solution to provide numerical estimates without sacrificing accuracy.

Problem for the Hydraulic Head

We consider an unconfined aquifer of infinite lateral extent and finite thickness that rests on an impermeable horizontal layer (Figure 1). The aquifer material is uniform and anisotropic, the principal conductivities being oriented parallel to the coordinate axes. The aquifer is recharged by a uniform circular source that is turned on at time zero. We neglect variations of specific yield. Within the limits of first-order linearized theory, the problem may be written as

$$K_h \frac{1}{\bar{r}} \frac{\partial}{\partial \bar{r}} \left(\bar{r} \frac{\partial \bar{s}}{\partial \bar{r}} \right) + K_v \frac{\partial^2 \bar{s}}{\partial \bar{z}^2} = S_s \frac{\partial \bar{s}}{\partial \bar{t}} \tag{1}$$

$$\bar{r} > 0 \qquad 0 < \bar{z} < 1 \qquad \bar{t} > 0$$

$$\lim_{\bar{r} \to \infty} \bar{s}(\bar{r}, \bar{z}, \bar{t}) = 0 \qquad \frac{\partial \bar{s}}{\partial \bar{r}}(0, \bar{z}, \bar{t}) = 0 \qquad \frac{\partial \bar{s}}{\partial \bar{z}}(\bar{r}, 0, \bar{t}) = 0 \tag{2}$$

$$K_v \frac{\partial \bar{s}}{\partial \bar{z}}(\bar{r}, b, \bar{t}) + S_y \frac{\partial \bar{s}}{\partial \bar{t}}(\bar{r}, b, \bar{t}) = IH(\bar{R} - \bar{r}) \tag{3}$$

$$H(x) = 1 \qquad x \geq 0$$
$$H(x) = 0 \qquad x < 0$$

$$\bar{s}(\bar{r}, \bar{z}, 0) = 0 \tag{4}$$

where $\bar{s}$ is the increase of hydraulic head over the initial value; $\bar{r}$, $\bar{z}$, and $\bar{t}$ are the radius, height above the bottom, and time; $\bar{R}$ is the radius of the circular source; b is the initial saturated thickness of the aquifer; K_h and K_v are the horizontal and vertical saturated hydraulic conductivities; S_s is the specific (elastic) storage; S_y is the specific yield; I is the net specific recharge at the water table; and H is the unit step function. (See *Dagan* [1967] and *Neuman* [1974] for the derivation of the model.) The recharge rate is taken to be steady for mathematical simplicity; the final results can be generalized for time-dependent recharge using the convolution theorem [*Sneddon*, 1972]. The bars are used to denote dimensional variables and parameters that will be replaced in the model by their dimensionless counterparts.

The equations are made dimensionless by introducing dimensionless variables that are scaled so as to simplify the equations and reduce the number of parameters in the problem from six ($\bar{R}$, b, K_h, K_v, S_s, S_y) to two. These new parameters represent the ratio of recharge area radius to aquifer depth and the compressibility (the ratio of specific elastic storage to specific yield) and are defined by

$$R = \frac{\bar{R}}{b} \left(\frac{K_v}{K_h} \right)^{1/2} \qquad \sigma = \frac{S_s b}{S_y} \tag{5}$$

To put the problem in dimensionless form, we choose b as the reference quantity for $\bar{z}$. Then to balance the spatial derivatives in the partial differential equation, we choose $b(K_h/K_v)^{1/2}$ as the reference quantity for $\bar{r}$. The reference quantity for $\bar{s}$ is chosen to be Ib/K_v to balance the source term and the vertical gradient term of (3). There are two choices for the time scale, depending on whether we balance the time derivative in the partial differential equation (1) or the time derivative in the recharge boundary condition (3). The first case gives the small time scale

$$t_s = S_s b^2/K_v \tag{6}$$

while the second case gives the large time scale

$$t_l = S_y b/K_v \tag{7}$$

Note that these scales are related by the equation $\sigma = t_s/t_l$. With these scales in mind, we define dimensionless variables by

$$z = \frac{\bar{z}}{b} \qquad r = \frac{\bar{r}}{b}\left(\frac{K_v}{K_h}\right)^{1/2} \qquad t = \frac{\bar{t}}{t_l} \qquad \tau = \frac{\bar{t}}{t_s} = \frac{t}{\sigma} \tag{8}$$

$$s(r, z, t) = (K_v/Ib)\ \bar{s}[\bar{r}(r), \bar{z}(z), \bar{t}(t)]$$
$$s(r, z, \tau) = (K_v/Ib)\ \bar{s}[\bar{r}(r), \bar{z}(z), \bar{t}(\tau)] \tag{9}$$

Depending on the choice of time scale, s may be considered as a function of (r, z, t) or (r, z, τ). The problem will look different on the two time scales.

In terms of the new variables the problem takes the form

$$\frac{1}{r}\frac{\partial}{\partial r}\left(r\frac{\partial s}{\partial r}\right) + \frac{\partial^2 s}{\partial z^2} = \sigma\frac{\partial s}{\partial t} \tag{10}$$

$$r > 0 \qquad 0 < z < 1 \qquad t > 0$$

$$\lim_{r\to\infty} s(r, z, t) = 0 \qquad \frac{\partial s}{\partial r}(0, z, t) = 0 \qquad \frac{\partial s}{\partial z}(r, 0, t) = 0 \tag{11}$$

$$\frac{\partial s}{\partial z}(r, 1, t) + \frac{\partial s}{\partial t}(r, 1, t) = H(R - r) \tag{12}$$

$$s(r, z, 0) = 0 \tag{13}$$

on the large time scale. On the small time scale the problem takes the form

$$\frac{1}{r}\frac{\partial}{\partial r}\left(r\frac{\partial s}{\partial r}\right) + \frac{\partial^2 s}{\partial z^2} = \frac{\partial s}{\partial \tau} \tag{14}$$

$$r > 0 \qquad 0 < z < 1 \qquad \tau > 0$$

$$\lim_{r\to\infty} s(r, z, \tau) = 0 \tag{15}$$

$$\frac{\partial s}{\partial r}(0, z, \tau) = 0 \qquad \frac{\partial s}{\partial z}(r, 0, \tau) = 0$$

$$\frac{\partial s}{\partial z}(r, 1, \tau) + \sigma^{-1}\frac{\partial s}{\partial \tau}(r, 1, \tau) = H(R - r) \tag{16}$$

$$s(r, z, 0) = 0 \tag{17}$$

No approximations have been used at this stage, so (10)–(13) and (14)–(17) are different versions of the exact problem. In section 3 we present the exact solution using the notation of the small time scale. In section 4 we present approximations valid on each time scale and a uniform approximation valid for all time.

Velocity Field

Once the increase of hydraulic head has been determined, the velocity field on any time scale can be obtained from the increase of hydraulic head by

$$\bar{V}_z = IV_z \qquad V_z = -\frac{\partial s}{\partial z} \tag{18}$$

$$\bar{V}_r = I\left(\frac{K_h}{K_v}\right)^{1/2} V_r \qquad V_r = -\frac{\partial s}{\partial r} \tag{19}$$

Note that the vertical velocity at the surface is approximately equal to the vertical velocity at the initial position of the water table ($z = 1$) [*Dagan*, 1967]. It can be obtained from the boundary condition (12) or (16) rather than by calculating the derivative directly from the solution $s(r, z, t)$ or $s(r, z, \tau)$.

3. Exact Solution

Increase of Hydraulic Head

Applying Hankel and Laplace transforms to the small time scale version of the problem (14)–(17) yields the solution

$$s = 2\sigma R\int_0^\infty J_o(yr)J_1(yR)\sum_{n=0}^{\infty}\omega_n(y, z, \tau)\,dy \tag{20}$$

where

$$\omega_o(y, z, \tau) = \psi_o(y)\chi_o(y, z)(1 - e^{-\tau(y^2 - \gamma_o^2)}) \tag{21}$$

$$\omega_n(y, z, \tau) = \psi_n(y)\chi_n(y, z)(1 - e^{-\tau(y^2 + \gamma_n^2)}) \tag{22}$$

$$n > 0$$

$$\psi_o(y) = \frac{\gamma_o^2}{(y^2 - \gamma_o^2)[\gamma_o^2(1 + \sigma) + y^2 - \sigma^{-1}(y^2 - \gamma_o^2)^2]} \tag{23}$$

$$\chi_o(y, z) = \frac{\cosh(\gamma_o z)}{\cosh\gamma_o}$$

$$\psi_n(y) = \frac{\gamma_n^2}{(y^2 + \gamma_n^2)[\gamma_n^2(1 + \sigma) - y^2 + \sigma^{-1}(y^2 + \gamma_n^2)^2]} \tag{24}$$

$$\chi_n(y, z) = \frac{\cos(\gamma_n z)}{\cos\gamma_n} \qquad n > 0$$

and the quantities $\gamma_n(y)$ are given implicitly by

$$\sigma\gamma_o\sinh\gamma_o - (y^2 - \gamma_o^2)\cosh\gamma_o = 0 \tag{25}$$

$$0 < \gamma_o < y$$

$$\sigma\gamma_n\sin\gamma_n + (y^2 + \gamma_n^2)\cos\gamma_n = 0 \tag{26}$$

$$(n - 1/2)\pi < \gamma_n < n\pi \qquad n > 0$$

Details of the computation appear in the appendix. The solution presented here is valid for all time and for all values of σ.

Vertical and Radial Velocities

Combining the exact solution for the hydraulic head with (19) and (18) gives the exact solutions for the dimensionless velocities:

$$V_z = -2\sigma R \int_0^\infty J_o(yr)J_1(yR) \sum_{n=0}^{\infty} \nu_n(y, z, \tau)\, dy \qquad (27)$$

$$V_r = 2\sigma R \int_0^\infty yJ_1(yr)J_1(yR) \sum_{n=0}^{\infty} \omega_n(y, z, \tau)\, dy \qquad (28)$$

where

$$\nu_o(y, z, \tau) = \psi_o(y) \frac{\gamma_o \sinh(\gamma_o z)}{\cosh \gamma_o} (1 - e^{-\tau(y^2 - \gamma_o^2)}) \qquad (29)$$

$$\nu_n(y, z, \tau) = -\psi_n(y) \frac{\gamma_n \sin(\gamma_n z)}{\cos \gamma_n} (1 - e^{-\tau(y^2 + \gamma_n^2)}) \qquad n > 0 \qquad (30)$$

The leading order approximation for the vertical velocity at the surface can also be obtained from the boundary condition (16) as

$$V_z(r, 1, \tau) = -H(R - r) + 2R \int_0^\infty J_o(yr)J_1(yR) \cdot \sum_{n=0}^{\infty} \frac{\partial \omega_n}{\partial \tau}(y, 1, \tau)\, dy \qquad (31)$$

Vertically Averaged Increase of Hydraulic Head

The increase of hydraulic head that is actually measured in an observation well perforated for elevations in the interval $z_1 < z < z_2$ (Figure 1) is the average of (20) over vertical distance and is thus given by the formula

$$\langle s \rangle_{z_1, z_2} = (z_2 - z_1)^{-1} \int_{z_1}^{z_2} s(r, z, \tau)\, dz \qquad (32)$$

By interchange of the limits of integration in the double integral defined by substitution of (20) into (32), one can obtain the average value as

$$\langle s \rangle_{z_1, z_2} = 2\sigma R \int_0^\infty J_o(yr)J_1(yR) \sum_{n=0}^{\infty} \langle \omega_n(y, \tau) \rangle\, dy \qquad (33)$$

where

$$\langle \omega_o(y, \tau) \rangle = \psi_o(y) \langle \chi_o(y) \rangle (1 - e^{-\tau(y^2 - \gamma_o^2)}) \qquad (34)$$

$$\langle \omega_n(y, \tau) \rangle = \psi_n(y) \langle \chi_n(y) \rangle (1 - e^{-\tau(y^2 + \gamma_n^2)}) \qquad (35)$$

$$\langle \chi_o(y) \rangle = \frac{\sinh(\gamma_o z_2) - \sinh(\gamma_o z_1)}{\gamma_o(z_2 - z_1) \cosh \gamma_o} \qquad (36)$$

$$\langle \chi_n(y) \rangle = \frac{\sin(\gamma_n z_2) - \sin(\gamma_n z_1)}{\gamma_n(z_2 - z_1) \cos \gamma_n} \qquad n > 0 \qquad (37)$$

4. Asymptotic Solution for $\sigma \ll 1$

Under the assumption $\sigma \ll 1$, asymptotic approximations to the solution of the problem for the increase of hydraulic head can be obtained as series in increasing powers of σ. The problems given by (10)–(13) and by (14)–(17) will give different asymptotic approximations because of differences in the way σ appears in the equations. An approximation valid on the large time scale (t_l) is called the outer expansion and can be obtained from the problem (10)–(13) by assuming a solution as a power series in σ, or it can be obtained from the exact solution by performing an asymptotic expansion of the solution for $\sigma \ll 1$ with t constant. An approximation valid on the small time scale (t_s) is called the inner expansion and can be obtained from the problem (14)–(17) by assuming a solution as a power series in σ, or it can be obtained from the exact solution by asymptotic expansion with τ constant. A uniformly valid approximate solution can be obtained from the inner and outer expansions by asymptotic matching [*Murdock*, 1991].

Because the inner and outer approximations are not valid for all time, they are used to replace the exact solution for further analysis. The uniform approximation is generally more complicated than either the outer or the inner approximation but can be used to replace the exact solution for numerical investigation.

Approximate Solution on the Small Time Scale

The inner approximation up to $O(\sigma)$ can be obtained from (14)–(17) by looking for a solution of the form

$$s^I = \sigma u(r, z, \tau) + O(\sigma^2) \qquad u = O(1) \qquad (38)$$

with $u(r, z, \tau)$ to be determined. The choice of $s = O(\sigma)$ is necessary so that the nonhomogeneous term in (16) remains in the equation in the limit $\sigma \to 0$. The spatial derivative term in the equation is thus small, with the consequence that this boundary condition can be integrated in time to yield

$$u(r, 1, \tau) = \tau H(R - r) \qquad (39)$$

From this analysis it is clear that at the beginning of the water recharge process, virtually all of the added water serves to produce a mound, and very little creates a downward flow of water.

The function $u(r, z, \tau)$ can be obtained directly from (14)–(17), with (39) replacing (16); however, it is easier to obtain the inner approximation s^I by asymptotic expansion of (20) as $\sigma \to 0$. The result is

$$s^I = \sigma R\tau \int_0^\infty J_o(yr)J_1(yR) \frac{\cosh yz}{\cosh y}\, dy - \sigma R \int_0^\infty J_o(yr)J_1(yR)F(y, z)\, dy - 2\sigma R \sum_{n=1}^{\infty} (-1)^n c_n \cos(c_n z) A_n(r, \tau) + O(\sigma^2) \qquad (40)$$

where

$$F(y, z) = \frac{\tanh y \cosh yz - z \sinh yz}{2y \cosh y} \tag{41}$$

$$A_n(r, \tau) = \int_0^\infty J_0(yr)J_1(yR)e^{-\tau(c_n^2 + y^2)} \frac{dy}{(c_n^2 + y^2)^2} dy$$

$$c_n = \left(n - \frac{1}{2}\right)\pi \qquad n > 0 \tag{42}$$

Details of the computation are available from the authors.

Approximate Solution on the Large Time Scale

Since σ is a small parameter, the outer approximation up to $O(1)$ can be obtained by setting $\sigma = 0$ in (10)–(13) and solving the resulting problem. Since the problem so obtained is the incompressible case, the result is that first demonstrated by *Dagan* [1967] using Green's functions:

$$s|_{\sigma = 0} \sim D(r, z, t) \equiv R \int_0^\infty J_o(yr)J_1(yR) \cdot (1 - e^{-ty \tanh y}) \frac{\cosh yz}{y \sinh y} dy \tag{43}$$

This solution can also be obtained by applying a Hankel transform, solving the resulting boundary value problem, and inverting the Hankel transform.

For the compressible case the outer solution can be approximated by an asymptotic series in powers of σ, with D as the leading order term. Up to $O(\sigma)$, the outer approximation is of the form

$$s^O = D(r, z, t) + \sigma\hat{s}(r, z, t) + O(\sigma^2) \tag{44}$$

where $\hat{s}$ is to be determined. The easiest way to obtain $\hat{s}$ is by expanding the exact solution (20) in powers of σ with t fixed. The result is

$$\hat{s} = -\frac{R}{2} \int_0^\infty J_o(yr)J_1(yR)\hat{\omega}(y, z, t) dy \tag{45}$$

where

$$\hat{\omega}(y, z, t) = e^{-ty \tanh y} [(t + 1) \tanh y + ty \operatorname{sech}^2 y - z \tanh yz] \frac{\cosh yz}{y \cosh y} \tag{46}$$

Note that $\hat{\omega}$ is always positive since the single negative term in the square brackets is always smaller than the first positive term, confirming that compressibility has the effect of decreasing the mound growth. Since this effect appears in the $O(\sigma)$ perturbation, it will be small on the large time scale.

Uniform Approximation to $O(\sigma)$

The approximation (40) is a valid approximation when $\bar{t} = O(t_s)$, while the approximation (44) is a valid approximation when $\bar{t} = O(t_l)$. To show the continuous dependence of the solution on time, a uniform approximation to the solution is needed. The uniform approximation is a combination of the inner and outer approximations constructed so that it reduces to the inner approximation for $\tau = O(1)$ and to the outer approximation for $t = O(1)$ and is also valid for intermediate times. The uniform approximation is obtained using the method of matched asymptotic expansions, as described by *Murdock* [1991]. The result is

$$s^U = s^O - 2\sigma R \sum_{n=1}^{\infty} (-1)^n c_n \cos (c_n z) A_n(r, \tau) + O(\sigma^2) \tag{47}$$

with the error $O(\sigma^2)$ for all time.

5. Long-Time ($t \to \infty$) Analysis of the Solution

Typical parameter values for shallow sand and gravel aquifers are $b = 10$ m, $K_v = 10$ m/d, and $S_y = 0.1$, giving a large time scale t_l of the order of 0.1 days.

Any study of the movement of groundwater over long recharge periods ($\bar{t} \geq 1$ day) will benefit from knowledge of the limiting behavior of the solution to the linearized problem as $t \to \infty$. This long-time behavior can be elucidated for both the incompressible and compressible cases using Laplace's method for the asymptotic expansion of integrals with a large parameter [*Bender and Orszag*, 1978]. The principal computational result is that the long-time behavior of an integral of the form

$$B(r, z, t, R) = \int_0^\infty \mathcal{K}(y, r, z, R)e^{-ty \tanh y} dy \tag{48}$$

where $\mathcal{K}$ has a power series expansion of the form

$$\mathcal{K}(y, r, z, R) = \sum_{n=n_o}^{\infty} k_n(r, z, R)y^{2n+1} \qquad n_o \geq 0$$

is given by

$$B = \frac{n_o!}{2} t^{-1-n_o} k_{n_o}(r, z, R) + O(t^{-2-n_o}) \tag{49}$$

provided $r, R = O(1)$.

Incompressible Case

The solution for the hydraulic head when $\sigma = 0$ is given by Dagan's formula (43). Although it is not possible to simplify this formula as $t \to \infty$, it is possible to obtain a simple result for the long-time behavior of s by examining the time derivative of Dagan's formula. From (43) and (49) comes the result

$$\left.\frac{\partial s}{\partial t}\right|_{\sigma = 0} = \frac{R^2}{4t} + O(t^{-2}) \qquad r, R = O(1) \tag{50}$$

Integration of this result yields

$$s = \frac{R^2}{4} \ln (t/t_o) + O(t^{-1}) \qquad r, R = O(1) \tag{51}$$

where t_0 is an integration constant that depends on r and z and can be approximated numerically.

From (43) and (49) the vertical and radial velocities are approximated by

$$V_z|_{\sigma=0} = -R\int_0^\infty J_o(yr)J_1(yR)\frac{\sinh yz}{\sinh y}\,dy + \frac{R^2 z}{4t} + O(t^{-2}) \qquad r, R = O(1) \tag{52}$$

$$V_r|_{\sigma=0} = R\int_0^\infty J_1(yr)J_1(yR)\frac{\cosh yz}{\sinh y}\,dy - \frac{R^2 r}{8t} + O(t^{-2}) \qquad r, R = O(1) \tag{53}$$

Note that the vertical velocity has a particularly simple form when $z = 1$. In this case the long-time approximation is easily obtained from (18), (12), and (50):

$$V_z(r, 1, t)|_{\sigma=0} = -H(R-r) + \frac{R^2}{4t} + O(t^{-2}) \qquad r, R = O(1) \tag{54}$$

Effect of Compressibility

To understand the long-time behavior of the solution s^O in (44) for the case where σ is small but not zero, it is sufficient to examine the behavior of the function $\hat{s}$ that is given by (45)–(46). Any additional compressibility effects will be much smaller, according to (44), and need not be considered.

To obtain an estimate of the effect of compressibility on the hydraulic head as $t \to \infty$, we note that from (45),

$$\hat{s} = -\left[\frac{Rt}{2} + O(1)\right]\int_0^\infty J_o(yr)J_1(yR)e^{-ty\tanh y}\cdot\frac{(\tanh y + y\,\mathrm{sech}^2 y)\cosh yz}{y\cosh y}\,dy$$

Thus from (49) we obtain the result

$$\hat{s} = -\frac{R^2}{4} + O(t^{-1}) \qquad r, R = O(1) \tag{55}$$

and then (using (51))

$$s = \frac{R^2}{4}[\ln(t/t_o) - \sigma] + O(t^{-1}) + O(\sigma^2) \qquad r, R = O(1) \tag{56}$$

For the effect of compressibility on the vertical velocity as $t \to \infty$ we may apply (49) to $-\partial\hat{s}/\partial z$, where $\hat{s}$ is given by (45). The result is

$$-\frac{\partial\hat{s}}{\partial z} = O(t^{-2}) \qquad r, R = O(1)$$

The long-time approximation for the vertical velocity is thus given by (52) even for the compressible case.

For the effect of compressibility on the radial velocity as $t \to \infty$ we apply (49) to

$$-\frac{\partial\hat{s}}{\partial r} = -\left[\frac{Rt}{2} + O(1)\right]\int_0^\infty J_1(yr)J_1(yR)e^{-ty\tanh y}\cdot\frac{(\tanh y + y\,\mathrm{sech}^2 y)\cosh yz}{\cosh y}\,dy$$

with the result

$$-\frac{\partial\hat{s}}{\partial r} = -\frac{R^2 r}{8t} + O(t^{-2}) \qquad r, R = O(1)$$

Combining this result with the incompressible case (53) gives the long-time approximation

$$V_r = R\int_0^\infty J_1(yr)J_1(yR)\cdot\frac{\cosh yz}{\sinh y}\,dy - (1+\sigma)\frac{R^2 r}{8t} + O(t^{-2}) \qquad r, R = O(1) \tag{57}$$

Dagan's solution thus slightly overestimates the radial velocity by an amount that is $O(\sigma t^{-1})$ as $t \to \infty$.

Formulas (56) and (57) show the quantitative effect of compressibility for very large times. Note that the effect of compressibility on the hydraulic head does not disappear with time (as reported for the well problem [*Neuman*, 1974] and subsequently corrected [*Gambolati*, 1976; *Neuman*, 1979]) but approaches a constant multiple of σ. The effect of compressibility on velocity does disappear with time.

6. Numerical Analysis and Discussion of Results

The previous sections provide exact and approximate formulas for the hydraulic head and flow velocities for incompressible and compressible aquifers according to the linearized theory and neglecting the effect of the unsaturated zone above the water table.

The examples and discussion that follows are motivated by two goals. The first is to give a description of the evolution of the groundwater mound and the velocity profile. The velocity profile is of particular importance since no results for the three-dimensional case have been published previously.

To simplify computations, one would like to use Dagan's formula to calculate vertical and radial velocities. Thus the second goal of the discussion is to indicate the effect of compressibility on the head and the velocities, since the use of Dagan's formula is tantamount to neglecting this effect.

To illustrate the solutions given by these formulas, the integrals in the formulas were evaluated numerically. The procedure is not entirely routine, because the integration interval is infinite and the integrands include two oscillating factors and have removable singularities at $y = 0$. To avoid these difficulties, the routine employed in these computations subdivided the y axis by placing a node at all points where the integrand vanished owing to the vanishing of an oscillatory factor, and each integral was evaluated on an interval $[\varepsilon, L]$ rather than the interval $[0, \infty]$. The very small positive number ε was chosen to avoid removable singularities at $y = 0$ (if necessary) without introducing significant error. The number L was chosen to be large enough so that

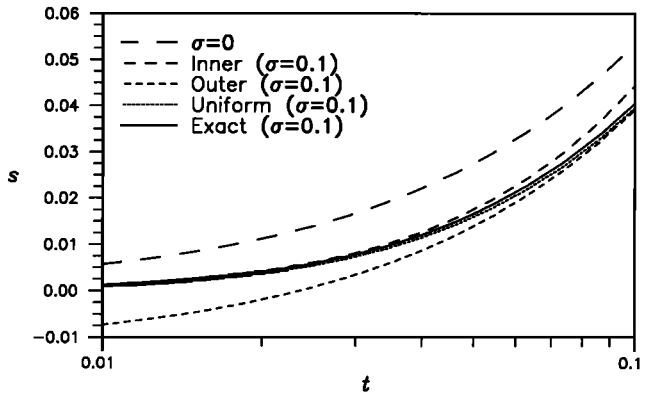

Fig. 2. Comparison of solutions for hydraulic head s for small times t, with $r = 0.5$ and $z = 0.5$.

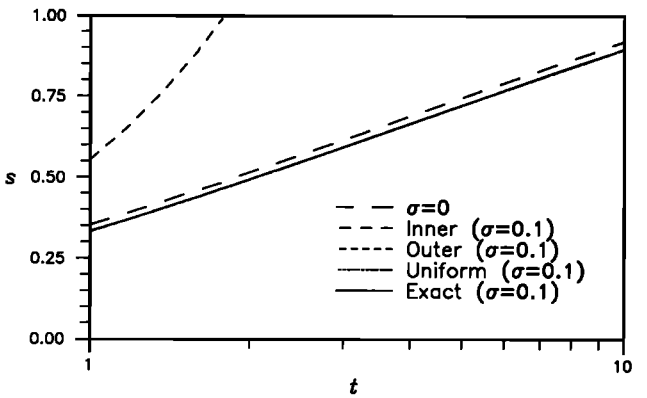

Fig. 4. Comparison of solutions for hydraulic head s for large times t, with $r = 0.5$ and $z = 0.5$.

the neglected interval $[L, \infty]$ did not make a noticeable contribution to the integral. Infinite sums were approximated by including enough terms to justify neglect of the remaining terms, and the implicitly defined functions $\gamma_n(y)$ were approximated using Newton's method. Programs in FORTRAN are available from the authors.

All numerical examples use $b = 10$ m, $K_v = 10$ m/d, and $S_y = 0.1$; a value of $t = 1$ then corresponds to the physical time $\bar{t} = 0.1$ days.

The ratio of source radius to saturated aquifer thickness (R) typically ranges from 0 to 10. For example, an isotropic sand and gravel aquifer 10 m thick with a center pivot irrigation system with 100-m radius gives $R = 10$. Numerical examples presented here take $R = 1$ as a convenient value for illustration.

Analysis of many pumping tests in different formations reported by *Neuman* [1979] yield values of σ that range from 0.001 to 0.01 and more. Larger values such as $\sigma = 0.2$ were obtained from sand tank experiments [*Neuman*, 1981]. These values are much larger than values calculated from the physical definition of the elastic storage coefficient S_s. An explanation was given by *Brutsaert and El-Kadi* [1984], who analyzed the relative importance of compressibility and partial saturation in unconfined groundwater flow and came to a quantitative conclusion about the role of σ. In many situations, flow processes in the unsaturated zone above the water table can be accounted for by employing a high effective value of σ, even though σ by definition is characteristic of the saturated zone under the water table.

The range of σ values can be even wider in the case of areal recharge sources that create vast zones of trapped air and unsaturated flow. We will use $\sigma = 0.1$ as an example corresponding to the upper range of σ values. Note that predictive applications of formulas derived above must use field data only for estimation of σ.

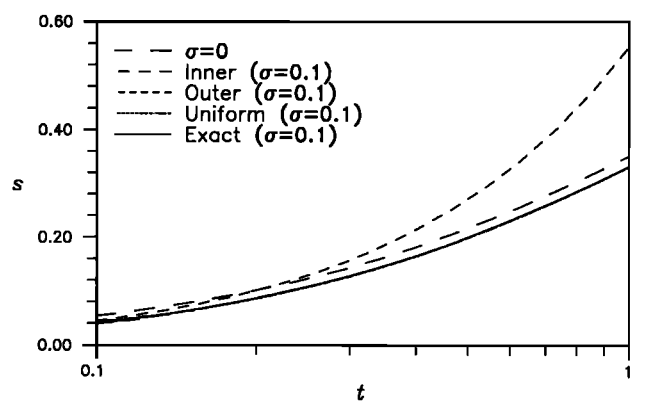

Fig. 3. Comparison of solutions for hydraulic head s for moderate times t, with $r = 0.5$ and $z = 0.5$.

Hydraulic Head

Figures 2–4 show a comparison of the various solutions and approximations for the hydraulic head at a typical point beneath the recharge area ($r = 0.5$, $z = 0.5$). Note that the incompressible solution may be considered as an approximation to the exact solution for the compressible case.

For small times (Figure 2) the uniform approximation is just distinguishable from the exact solution. The absolute difference is small because insufficient time has elapsed for a significant increase in the hydraulic head, and both solutions start with a head increase of zero. The inner approximation gives a good representation of the solution up to the time 0.05 (corresponding to $\tau = 0.5$) but begins to diverge after that. Dagan's formula shows the correct trend in a qualitative sense, but without quantitative accuracy. The outer approximation is actually negative and therefore meaningless. (Since the outer approximation is obtained under the assumption that $t = O(1)$, there is no reason to expect it to be valid near $t = 0$.)

For intermediate times (Figure 3) the uniform and outer approximations are indistinguishable from the exact solution. Note that the difference between the uniform and outer approximations is given by the exponentially decaying term of the inner solution (40), which is virtually 0 even for $\tau = 1$. Dagan's formula overestimates the hydraulic head by an amount that is growing only slowly with time and appears to be approaching a constant deviation ($-\sigma R^2/4 = 0.25$), in accordance with the analysis of (56).

For large times (Figure 4) the trends established in the intermediate range are continued, with the deviation of Dagan's formula from the correct solution approximately constant.

The vertically averaged hydraulic head is illustrated in Figure 5 at various radii. The graph shows the approach of the deviation of Dagan's formula from the compressible

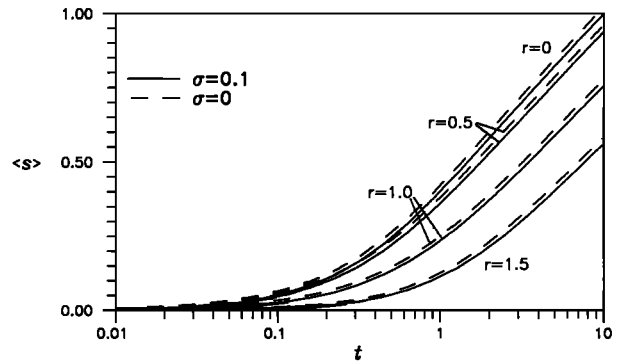

Fig. 5. The vertically averaged hydraulic head $\langle s \rangle$ at various radii r as a function of time t.

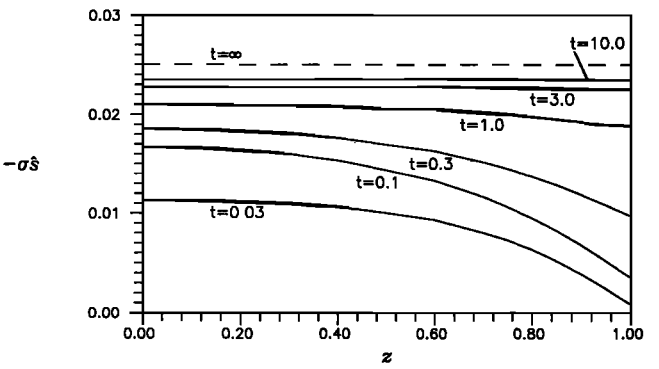

Fig. 7. Correction (due to compressibility) to the incompressible hydraulic head as a function of depth z, with $r = 0$.

solution to a constant as t increases, and it shows the approach to a logarithmic increase with time for $t > 1$.

Figure 6 shows how the variation of hydraulic head with depth at the center of the recharge area changes with time. As the flow evolves, vertical gradients in head increase, leading to larger downward velocity.

The effect of compressibility increases with t and decreases with r and z. The increase in the effect of compressibility with r is immediately obvious from the observation that the integrand of the function $\hat{s}$ (45) achieves its maximum magnitude at $r = 0$ for any value of y. The decrease of compressibility effect with z diminishes with time, while the overall effect of compressibility reaches a limiting value as time increases (Figure 7 and (56)). The reason for this behavior is clear from the asymptotic results. The inner approximation (40) consists of three terms. The first of these corresponds to Dagan's solution on the small time scale. The other two terms give the effect of compressibility. Of these, the third term decays rapidly, so that the principal small-time effect of compressibility is given by the second term. This function vanishes when $z = 1$, so that the effect of compressibility is small near the water table. As time increases to large values, the difference between the hydraulic head in compressible and incompressible aquifers is seen to approach the constant value $-\sigma R^2/4$.

Dagan's solution clearly gives a better approximation to the compressible solution for large times than for small times under most circumstances, as seen from examination of the inner and outer approximations (40) and (44). In the inner solution the term corresponding to Dagan's solution is just one of three leading order terms. There is no reason to expect the behavior of the compressible solution to resemble that of the incompressible solution very closely for small times. However, as time increases, the term corresponding to Dagan's solution increases, the second term in the inner approximation remains $O(\sigma)$, and the third term decays rapidly to 0. In the outer approximation, Dagan's solution is the only leading order term, so that for σ sufficiently small we may regard Dagan's solution as being exactly correct on the large time scale.

Figure 8 shows the variation of hydraulic head with radius at the water table, with $z = 1$. Since the hydraulic head at the water table represents the change in water table elevation due to recharge, this figure illustrates the evolution of the groundwater mound caused by recharge. For small times the groundwater mound is essentially a step function, with a uniform rise in head under the recharge area. This behavior was predicted by the boundary condition (16) at the surface on the small time scale. Since the head is $O(\sigma)$, the boundary condition says that in the initial stage of recharge, virtually all of the water added to the system goes into the building of the mound (the time derivative term) rather than into the development of downward flow (the spatial derivative term). As time increases, the shape of the mound becomes smooth.

Vertical Velocity

Figures 9–12 show the radial distribution of downward velocity for different times (t = 0.01, 0.1, 1.0, and 10.0,

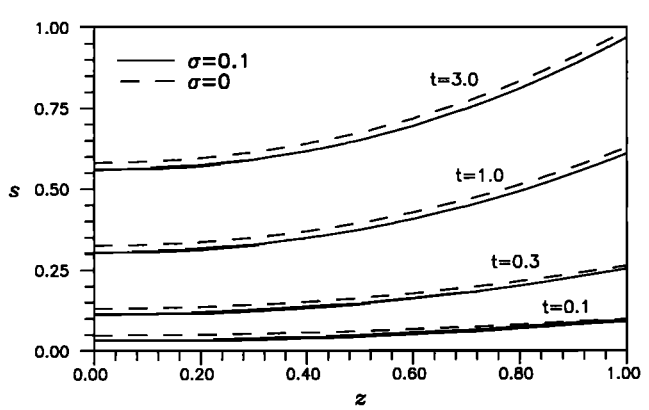

Fig. 6. Variation of hydraulic head s with depth z at various times t, with $r = 0$.

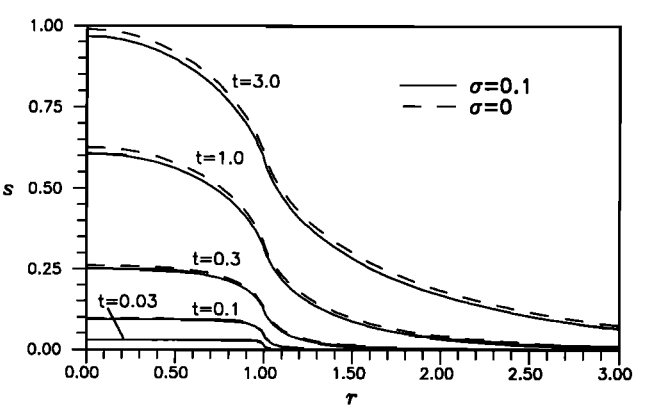

Fig. 8. Variation of hydraulic head s with radius r at various times, with $z = 1$.

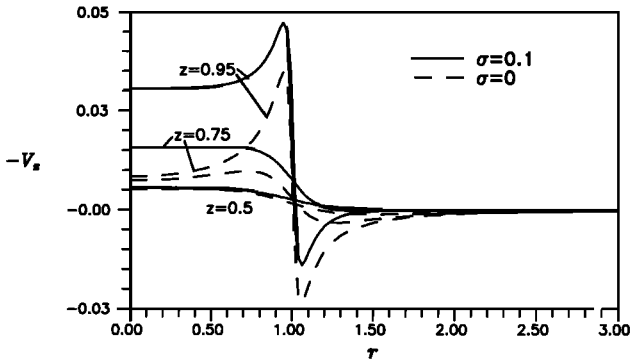

Fig. 9. Variation of downward velocity $-V_z$ with radius r at various depths z, with $t = 0.01$.

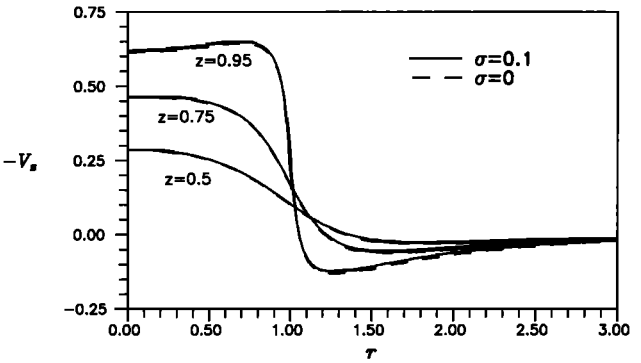

Fig. 11. Variation of downward velocity $-V_z$ with radius r at various depths z, with $t = 1.0$.

respectively). Each graph shows the vertical velocity at the depths given by $z = 0.95$, $z = 0.75$, and $z = 0.5$. The vertical velocity at the bottom of the aquifer is zero. The vertical velocity is not a monotonic function of radius. Because there is no recharge outside of the circle $r = R$, water which enters the aquifer near the edge of the recharge area can move outward as well as downward; hence the downward velocity near the water table is greatest at the edge of the recharge area. The downward flow of water near $r = R$ creates a region just outside the recharge area where the head increases with increasing depth, creating the upward flow of water seen for $r > R$. This effect diminishes with depth and diminishes also with time. Eventually, for $t \gg 1$, the profile becomes a monotonic function of the radius r at any depth. Figure 13 shows the downward velocity at the water table, which approaches a step function as time increases, in accordance with (54).

For small times ($t \ll 1$) the difference between compressible and incompressible aquifers is significant. Figure 9 shows that compressibility causes an increase in downward velocity in the earliest stage of recharge. The effect of compressibility is to retard the propagation of spatial hydraulic head differences from the source of the perturbation down the aquifer. This gives a larger vertical gradient of hydraulic head than in the incompressible case. Thus for small times, Dagan's formula is adequate for the vertical velocity near the bottom of the aquifer but gives a result which is much too low for the downward velocity near the water table.

The error in Dagan's solution diminishes rapidly with time. The third term of the inner solution (43), which is the largest term for τ near zero, becomes small even for $\tau = 1$, so that its effect is rapidly lost. For large times ($t \gg 1$) the error in Dagan's formula is essentially zero, as (52) represents an excellent approximation to the vertical velocity for the compressible case as well as the incompressible case. Thus Dagan's formula may be safely used for $t > 1$. Moreover, it can be used to provide velocity estimates for particle tracking methods since the absolute error of time integrals of vertical velocity becomes stabilized after intermediate times.

Radial Velocity

Figures 14–16 show the evolution of the radial distribution of radial velocity at the depths given by $z = 0.95$, 0.75, and 0, respectively. Note that at any depth the radial velocity shows an absolute maximum at the edge of the recharge area. The gradient of the radial velocity is large near the water table but diminishes with depth. Indeed, the radial velocity at the water table below the edge of the recharge area cannot be computed because the integral for radial velocity diverges at $r = R$. The graphs also show that the effect of compressibility on the radial velocity is always small near the water table and is small at all depths for large times.

The effect of compressibility on the radial velocity is rather small, so that with the exception of the point $r = R$, $z = 1$, where Dagan's formula cannot be used, the use of Dagan's formula for the compressible case is justified. In the

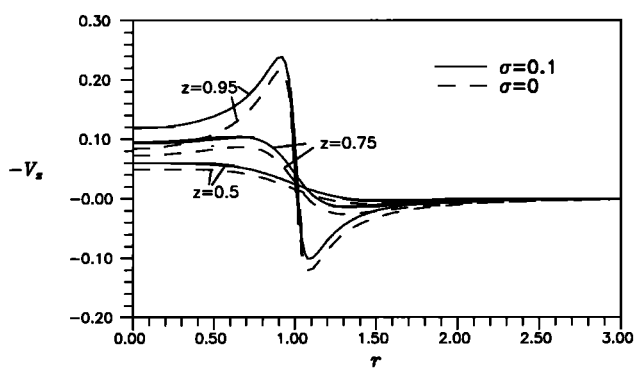

Fig. 10. Variation of downward velocity $-V_z$ with radius r at various depths z, with $t = 0.1$.

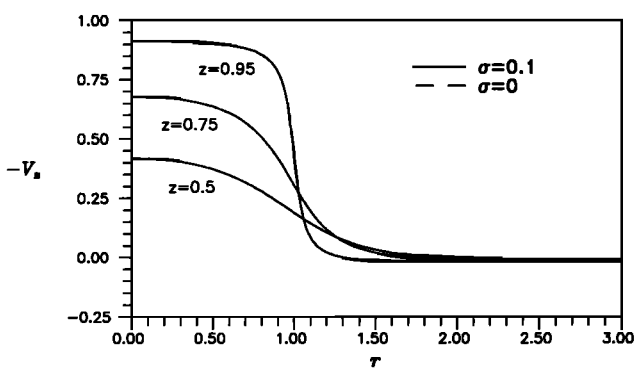

Fig. 12. Variation of downward velocity $-V_z$ with radius r at various depths z, with $t = 10.0$.

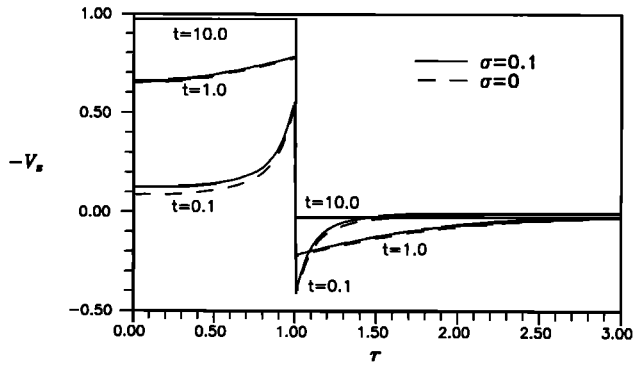

Fig. 13. Downward velocity $-V_z$ at the water table ($z = 1$) as a function of radius r at various times t.

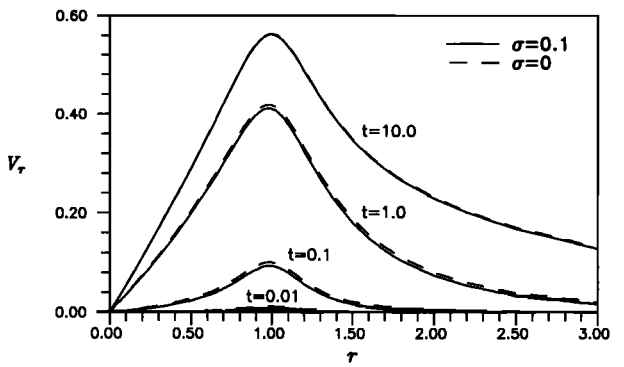

Fig. 15. Variation of radial velocity V_r with radius r at $z = 0.75$ at various times t.

upper levels of the aquifer, Dagan's formula gives good results for the radial velocity even for small times. At the bottom of the aquifer, Dagan's formula gives a larger radial velocity for small times. This effect occurs because changes in the hydraulic head propagate toward the bottom of the aquifer at a slower rate for the compressible case than for the incompressible case.

The error in using Dagan's formula for the radial velocity will not be important in problems of contaminant transport. Contaminants that are present near the water table at the beginning of the recharge (at time $\tau = 0$) will not reach the lower levels of the aquifer until the time is large enough for Dagan's formula to give an accurate estimate for the radial velocity near the bottom.

The overall direction of groundwater flow is apparent by comparison of the illustrations of the vertical and radial velocities. For the portion of the aquifer that is well within the recharge area ($r < R$, $r \neq R$), the radial velocity is small and the flow is primarily downward. For the portion of the aquifer that is well outside the recharge area the vertical velocity is small and the flow is primarily outward.

Importance of σ and R

For all quantities of interest the error in Dagan's formula as an estimate of the solution for the compressible case is proportional to σ. Thus for aquifers where σ is less than 0.1, the value used for all illustrations, the error in Dagan's formula is reduced accordingly.

It is interesting to note that all estimates of the effect of compressibility for large times are proportional to (σR^2). Since R is the ratio of the recharge radius to the aquifer depth, we conclude that for a given recharge area the effect of compressibility is less for a deep aquifer, which will have a small value of R, than for a shallow aquifer. Thus Dagan's formula makes a smaller absolute error for a deep aquifer than for a shallow aquifer.

7. Conclusions

In contrast with most previous works on transient groundwater flow in an unconfined aquifer under uniform recharge, compressibility of the aquifer has been taken into account analytically. The solution obtained from this analysis generalizes *Dagan*'s [1967] solution for the hydraulic head, which was derived by neglecting the compressibility.

By treating the compressibility σ, the ratio of storativity to specific yield, as a small parameter, further analysis of the solution for the hydraulic head in a compressible aquifer was performed by asymptotic methods, resulting in approximations to the exact solutions for head, vertical velocity, and radial velocity on small and large time scales and also in the limit of very large time.

It was found that Dagan's solution for the hydraulic head always overpredicts the growth of the groundwater mound. For large times the error in Dagan's formula does not depend on the location of the observation point or on the time and is equal to the constant value $-\sigma R^2/4$.

For small times ($\bar{t} < t_l$, where t_l is of the order of 1–10 hours) the profile of the vertical velocity at any depth $z > 0$ demonstrates that beyond the edge of the recharge area the

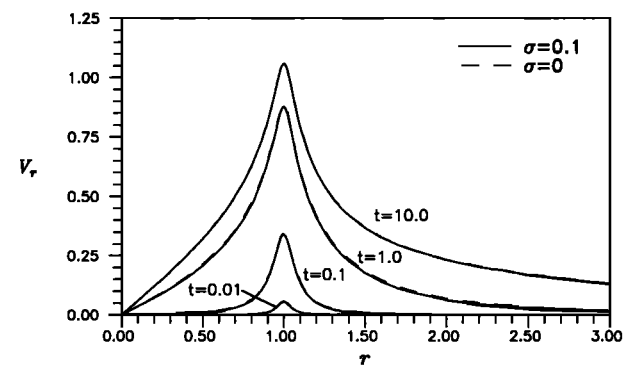

Fig. 14. Variation of radial velocity V_r with radius r at $z = 0.95$ at various times t.

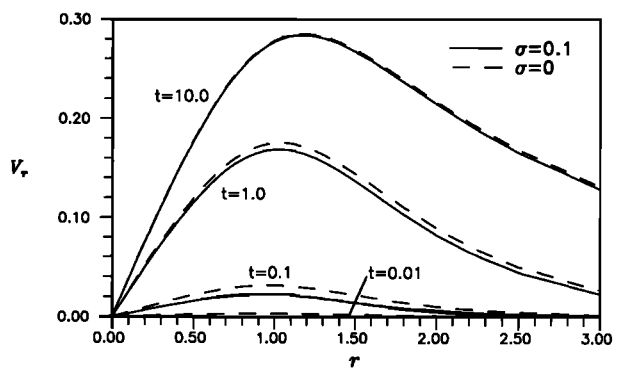

Fig. 16. Variation of radial velocity V_r with radius r at $z = 0$ at various times t.

flow of water is directed upward rather than downward. During this early period the compressibility of an aquifer may have a significant influence on hydraulic heads, water table shape, and velocities.

After $\bar{t} = t_l$ the vertical velocity gradually becomes a monotonic function of the radius r; in particular, the vertical velocity near the water table approaches a step function. Nonsteady components of the vertical and radial velocities show a decrease inversely proportional to time. The effect of compressibility on the velocities decreases after $\bar{t} = t_l$. For large times ($\bar{t} \gg t_l$) the error in the radial velocity caused by neglecting compressibility is inversely proportional to $\bar{t}$, while the error for vertical velocity is inversely proportional to $\bar{t}^2$.

Thus application of Dagan's formula to approximate flow in a compressible aquifer provides a very reasonable approximation for $\bar{t} > t_l$. For $\bar{t} < t_l$ the relative error in Dagan's formula can be significant for an aquifer with $\sigma \approx 0.1$, but the absolute error is always small. This makes Dagan's formula an attractive choice for the calculation of three-dimensional velocity fields for various particle tracking techniques and transport problems, where velocities are to be integrated over times of at least t_l.

APPENDIX: DERIVATION OF THE EXACT SOLUTION

For any function $f(r, z, \tau)$ we define $f^*(y, z, \tau)$ to be the Hankel transform of f, and for any function $f^*(y, z, \tau)$ we define $\bar{f}^*(y, z, p)$ to be the Laplace transform of f^* [*Sneddon*, 1972; *Neuman*, 1974]:

$$f^*(y, z, \tau) = \int_0^\infty J_o(yr) f(r, z, \tau) r \, dr$$

$$f(r, z, \tau) = \int_0^\infty J_o(yr) f^*(y, z, \tau) y \, dy \tag{58}$$

$$\bar{f}^*(y, z, p) = \int_0^\infty e^{-p\tau} f^*(y, z, \tau) \, d\tau$$

$$f^*(y, z, \tau) = \frac{1}{2\pi i} \int_{\gamma - i\infty}^{\gamma + i\infty} e^{p\tau} \bar{f}^*(y, z, p) \, dp \tag{59}$$

Applying Hankel and Laplace transforms to (14)–(17) yields the boundary value problem

$$\frac{\partial^2 \bar{s}^*}{\partial z^2} - (y^2 + p)\bar{s}^* = 0$$

$$\frac{\partial \bar{s}^*}{\partial z}(y, 0, p) = 0$$

$$\frac{\partial \bar{s}^*}{\partial z}(y, 1, p) + \sigma^{-1} p \bar{s}^*(y, 1, p) = \frac{RJ_1(yR)}{yp}$$

The solution of this problem is

$$\bar{s}^* = \frac{\sigma R J_1(yR)}{y} \bar{g}(y, z, p)$$

where

$$\bar{g} = \frac{\cosh(\eta z)}{p(\sigma\eta \sinh \eta + p \cosh \eta)} \qquad \eta = \sqrt{y^2 + p}$$

Inversion of the Laplace transform (59) yields

$$s^*(y, z, \tau) = \frac{\sigma R J_1(yR)}{y} g(y, z, \tau)$$

$$g = \frac{1}{2\pi i} \int_{\gamma - i\infty}^{\gamma + i\infty} e^{p\tau} \bar{g}(y, z, p) \, dp$$

and inversion of the Hankel transform (58) then yields

$$s(r, z, \tau) = \sigma R \int_0^\infty J_o(yr) J_1(yR) g(y, z, \tau) \, dy \tag{60}$$

To complete the solution, one needs only to compute the function $g(y, z, \tau)$. The initial condition (17) yields the result $s^*(y, z, 0) = 0$, from which we see that $g(y, z, 0) = 0$. Hence we may obtain g from the modified equation [*Neuman*, 1974]

$$g(y, z, \tau) = \frac{1}{2\pi i} \int_{\gamma - i\infty}^{\gamma + i\infty} G(p) \, dp = \sum \text{Res}\{G(p), p_n\} \tag{61}$$

where

$$G(p) = \frac{\phi[p, \eta(p)]}{\psi[\eta(p)]} \qquad \eta^2 = y^2 + p$$

$$\phi(p, \eta) = (e^{p\tau} - 1)p^{-1} \cosh(\eta z)$$

$$\psi(\eta) = \sigma\eta \sinh \eta + (\eta^2 - y^2) \cosh \eta$$

and Res $\{G(p), p_n\}$ is the residue of G at the pole p_n. The poles of G are the roots of the equation

$$\psi[\eta(p)] = 0 \tag{62}$$

since the function ϕ has only a removable singularity. It is known [*Neuman*, 1974] that (62) has one real root and an infinite number of imaginary roots:

$$\eta_o = \gamma_o(y), \text{ and } \eta_n = i\gamma_n(y) \qquad n = 1, 2, \ldots \tag{63}$$

where the real functions γ_n are given implicitly by

$$\sigma\gamma_o \sinh \gamma_o - (y^2 - \gamma_o^2) \cosh \gamma_o = 0 \qquad 0 < \gamma_o < y$$

$$\sigma\gamma_n \sin \gamma_n + (y^2 + \gamma_n^2) \cos \gamma_n = 0$$

$$(n - 1/2)\pi < \gamma_n < n\pi \qquad n > 0$$

The calculation of residues can be performed by [*Churchill and Brown*, 1984]

$$\text{Res}\left\{\frac{\phi[p, \eta(p)]}{\psi[\eta(p)]}, p_n\right\} = \frac{\phi[p_n, \eta(p_n)]}{\frac{d\psi}{dp}[\eta(p_n)]} = \frac{2\eta_n \phi(p_n, \eta_n)}{\frac{d\psi}{d\eta}(\eta_n)}$$

Hence

$$g(y, z, \tau) = 2 \sum_{n=0}^{\infty} \omega_n(y, z, \tau), \quad \omega_n = \frac{\eta_n \phi(p_n, \eta_n)}{\frac{d\psi}{d\eta}(\eta_n)} \tag{64}$$

With

$$\phi(p_n, \eta_n) = \frac{e^{p_n \tau} - 1}{p_n} \cosh(\eta_n z)$$

$$= \frac{1 - e^{-\tau(y^2 - \eta_n^2)}}{y^2 - \eta_n^2} \cosh(\eta_n z)$$

$$\frac{d\psi}{d\eta}(\eta_n) = \eta_n^{-1}[\eta_n^2(1+\sigma) + y^2 - \sigma^{-1}(y^2 - \eta_n^2)^2] \cosh \eta_n$$

and η_n given by (63), the final result (20) is given by (60) and (64).

NOTATION

b	initial saturated thickness of the aquifer.
$D(r, z, t)$	Dagan's solution for s for an incompressible aquifer.
H	unit step function.
I	net specific recharge at the water table.
J_0	Bessel function of the first kind of order 0.
J_1	Bessel function of the first kind of order 1.
K_h	horizontal hydraulic conductivity.
K_v	vertical hydraulic conductivity.
$r, \bar{r}$	dimensionless and dimensional radius.
$R, \bar{R}$	dimensionless and dimensional radius of recharge area.
$s, \bar{s}$	dimensionless and dimensional increase of hydraulic head over its initial value.
$\langle s \rangle$	vertical average of s from $z = 0$ to $z = 1$.
$\langle s \rangle_{z_1, z_2}$	vertical average of s from z_1 to z_2.
s^I	inner (small time) approximation to s for small σ.
s^O	outer (large time) approximation to s for small σ.
s^U	uniform approximation to s for small σ.
S_s	specific (elastic) storage.
S_y	specific yield.
t	dimensionless time on the large time scale.
$\bar{t}$	dimensional time.
t_l	large time scale.
t_s	small time scale.
V_r	dimensionless radial velocity.
V_z	dimensionless vertical velocity.
$z, \bar{z}$	dimensionless and dimensional distance from the bottom of the aquifer.
σ	compressibility parameter.
τ	dimensionless time on the small time scale.

Acknowledgment. The present work was partially supported by the Water Center of the University of Nebraska—Lincoln and the MSEA project.

REFERENCES

Bender, C. M., and S. A. Orszag, *Advanced Mathematical Methods for Scientists and Engineers*, McGraw-Hill, New York, 1978.

Brutsaert, W., and A. I. El-Kadi, The relative importance of compressibility and partial saturation in unconfined groundwater flow, *Water Resour. Res.*, *20*(3), 400–408, 1984.

Churchill, R. V., and J. W. Brown, *Complex Variables and Applications*, 4th ed., McGraw-Hill, New York, 1984.

Dagan, G., Linearized solutions of free-surface groundwater flow with uniform recharge, *J. Geophys. Res.*, *72*(4), 1183–1193, 1967.

Dillon, P. J., An analytical model of contaminant transport from diffuse sources in saturated porous media, *Water Resour. Res.*, *25*(6), 1208–1218, 1989.

Gambolati, G., Transient free surface flow to a well: An analysis of theoretical solutions, *Water Resour. Res.*, *12*(1), 27–39, 1976.

Hantush, M. S., Growth and decay of groundwater-mounds in response to uniform percolation, *Water Resour. Res.*, *3*(1), 227–234, 1967.

Hunt, B. W., Vertical recharge of unconfined aquifers, *J. Hydraul. Div. Am. Soc. Civ. Eng.*, *97*(7), 1017–1030, 1971.

Kroszinksy, U. I., and G. Dagan, Well pumping in unconfined aquifers: The influence of the unsaturated zone, *Water Resour. Res.*, *11*(3), 479–490, 1975.

Lennon, G. P., L.-F. Liu, and J. A. Ligget, Boundary integral equation solution to axisymmetric potential flows, 2, Recharge and well problems, *Water Resour. Res.*, *15*(5), 1107–1115, 1979.

Levy, B. S., P. J. Riordan, and R. Schreiber, Estimation of leak rates from underground storage tanks, *Ground Water*, *28*(3), 378–384, 1990.

Morel-Seytoux, H. J., C. Mirzacapillo, and M. J. Abdulrazak, A reductionist approach to a unsaturated aquifer recharge from a circular spreading basin, *Water Resour. Res.*, *26*(4), 771–777, 1990.

Murdock, J. A., *Perturbations: Theory and Methods*, 509 pp., John Wiley, New York, 1991.

National Research Council, *Ground Water Models: Scientific and Regulatory Applications*, 333 pp., Committee on Ground Water Modeling Assessment, Water Science and Technology Board, Commission on Physical Sciences, Mathematics, and Resources, National Academy Press, Washington, D. C., 1990.

Neuman, S. P., Effect of partial penetration on flow in unconfined aquifers considering delayed gravity response, *Water Resour. Res.*, *10*(2), 303–312, 1974.

Neuman, S. P., Analysis of pumping test data from anisotropic unconfined aquifers considering delayed gravity response, *Water Resour. Res.*, *11*(2), 329–342, 1975.

Neuman, S. P., Perspective on "delayed yield," *Water Resour. Res.*, *15*(4), 899–908, 1979.

Neuman, S. P., Delayed drainage in a stream-aquifer system, *J. Irrig. Drain. Div. Am. Soc. Civ. Eng.*, *107*(IR4), 407–410, 1981.

Ostendorf, D. W., D. A. Reckhow, and D. J. Popielarczyk, Vertical transport processes in unconfined aquifers, *J. Contam. Hydrol.*, *4*, 93–107, 1989.

Sneddon, I. H., *The Use of Integral Transforms*, McGraw-Hill, New York, 1972.

G. Ledder, Department of Mathematics, University of Nebraska, Lincoln, NE 68588.

V. Zlotnik, Department of Geology, University of Nebraska, Lincoln, NE 68588.

(Received May 29, 1991;
revised February 6, 1992;
accepted February 20, 1992.)